A Synthesis Technique of Time-Domain Interconnect Models by MIMO Type of Selective Orthogonal Least-Square Method

Masaya Suzuki, Hirofumi Miyashita, Atsushi Kamo, Takayuki Watanabe, *Member, IEEE*, and Hideki Asai, *Member, IEEE*

***Abstract*—This paper describes an efficient synthesis technique of time-domain models for interconnects characterized by sampled data. In this method, poles are derived from the sampled data in the frequency domain. Next, the dominant poles and the residues are obtained efficiently by multiinput–multioutput type of selective orthogonal least-square method. Furthermore, time-domain models are derived from the frequency-domain models. Finally, the accuracy and efficiency of the proposed method are substantiated by transient simulation of example circuits using this model.**

***Index Terms*—FDTD method, high-speed interconnect analysis, MIMO type of approximation, model reduction, selective orthogonal least-square method.**

I. Introduction

THE development of very large scale integration (VLSI) circuit technology is yielding larger chips with smaller and faster devices. As a result, interconnect effects such as signal delay, reflection, and crosstalk can severely degrade the signal integrity on the printed circuit board (PCB). Therefore, transmission-line models should be used in order to simulate the transient responses of interconnects accurately.

One-dimensional transmission-line models have been widely used in the time-domain simulation [1]–[4]. However, these models usually assume the ideal ground and take no account of physical structures. Therefore, these models cannot provide the electromagnetic effects on the PCB accurately. To estimate those effects of high-speed interconnects accurately, it is necessary to perform full-wave analysis such as the finite-difference time-domain (FDTD) method [5]–[7] and finite-element method (FEM), or measurement by high-performance instruments. However, computational cost of such simulation is usually much more expensive compared with the analysis of lumped networks. Therefore, several methods to synthesize the macromodel with poles and residues obtained from sampled data in the frequency domain, which can be calculated by full-wave analysis (or measurement) and fast Fourier transform (FFT), have been proposed [8]–[16]. Once these macromodels have been formed, the circuit equations can be set up by the standard approaches for the systematic formulation underlying a circuit solver like the modified nodal analysis (MNA).

In these modeling techniques, the rational functions are usually approximated from sampled data using the least-square method, and the poles are derived. Although the least-square method is an effective method when the sampled data are obtained within a narrow bandwidth, this method suffers from a singularity problem for the wide bandwidth. If the frequency range in electromagnetic-field analysis is more than 10 GHz, the least-square method is insufficient to model the interconnects accurately. To overcome this problem, the frequency range had better be divided into several regions and, in each region, is approximated by using poles and residues, where only the dominant poles have to be selected because remaining poles contain some undesirable poles such as unstable ones. Complex frequency hopping (CFH) is one of the methods that selects the dominant poles from the several frequency regions [2]. However, this method is sometimes heuristic, hard to apply automatically, and may be computationally expensive. On the other hand, for selection of the desirable poles, an adaptive least-square method has been proposed [13], which is the single-input–single-output (SISO) method. Since the poles and residues of each element are calculated separately, the simulation cost increases for the modeling of multiport circuits.

In this paper, we propose an efficient model order-reduction technique for circuits formulated in terms of Y-parameters [17] by a multiinput–multioutput (MIMO) type of selective orthogonal least-square (SOLS) method. First, approximation of the frequency response is described in Section II, where the frequency region is divided into several regions and the transfer function for each region is approximated with poles and residues from sampled data. Next, a technique for selection of the dominant poles by a MIMO type of SOLS method is proposed in Section III, and synthesis of the time-domain model is shown in Section IV. In Section V, some numerical results are given. Section VI provides some conclusions.

II. Approximation of the Frequency Response

In this section, the method to derive a transfer function with poles and residues from sampled data, which is the admittance matrix, is described.

Manuscript received January 15, 2000. This work was supported in part by a Grant-in-Aid for Scientific Research of the Ministry of Education, Science and Culture of Japan under grants (C).

M. Suzuki, A. Kamo, and H. Asai are with the Department of Systems Engineering, Shizuoka University, Hamamatsu 432-8561, Japan (e-mail: hideasai@sys.eng.shizuoka.ac.jp).

H. Miyashita was with the Department of Systems Engineering, Shizuoka University, Hamamatsu 432-8561, Japan. He is now with the Matsushita Electric Industrial Company Ltd., Kadoma, Osaka 571-8501, Japan.

T. Watanabe is with the School of Administration and Informatics, University of Shizuoka, Hamamatsu 432-8561, Japan.

Publisher Item Identifier S 0018-9480(01)08687-2.

To approximate each element Y_{ij} of the admittance matrix, we use a rational function of the form

$$Y_{ij}(s) = \frac{b_0 + b_1 s + b_2 s^2 + \cdots + b_m s^m}{1 + a_1 s + a_2 s^2 + \cdots + a_n s^n} \tag{1}$$

where the coefficients a_i and b_i are approximated by using least-square approximation. In this case, these coefficients can be obtained by fitting it to the calculated sampled data

$$Y_{ij}(s_q) = \frac{b_0 + b_1 s_q + b_2 s_q^2 + \cdots + b_m s_q^m}{1 + a_1 s_q + a_2 s_q^2 + \cdots + a_n s_q^n}, \qquad q = 1, \ldots, H \tag{2}$$

where H is the number of frequency points. However, if the bandwidth to be approximated is too wide, the least-square method does not give reliable results; that is to say, the rational function may include unstable poles in the right half-plane and have large truncation errors. To overcome this problem, the frequency region is divided into some regions, and the frequency response at each region is separately approximated by the rational function (2) [8]. Therefore, the least-square equation can be derived in each region as follows:

$$(\boldsymbol{X}^T \boldsymbol{X}) \cdot \boldsymbol{c} = \boldsymbol{X}^T \boldsymbol{f} \tag{3}$$

where

$$\boldsymbol{X} = \begin{bmatrix} 1 & s_1 & \cdots & s_1^m & -Y_{ij}(s_1)s_1 & \cdots & -Y_{ij}(s_1)s_1^n \\ 1 & s_2 & \cdots & s_2^m & -Y_{ij}(s_2)s_2 & \cdots & -Y_{ij}(s_2)s_2^n \\ \vdots & \vdots & & \vdots & \vdots & & \vdots \\ 1 & s_L & \cdots & s_L^m & -Y_{ij}(s_L)s_L & \cdots & -Y_{ij}(s_L)s_L^n \end{bmatrix}$$

$$\boldsymbol{c} = \begin{bmatrix} b_0 & \cdots & b_m & a_0 & \cdots & a_n \end{bmatrix}^T$$

$$\boldsymbol{f} = \begin{bmatrix} Y_{ij}(s_1) & Y_{ij}(s_2) & \cdots & Y_{ij}(s_n) \end{bmatrix}^T$$

where L is the number of frequency points in each region. Actually, (3) can be solved by the QR decomposition technique to improve the accuracy of the least-square method. $\boldsymbol{QR}$ transformation decomposes a square matrix into theproduct of an orthogonal matrix $\boldsymbol{Q}$ and a right triangular matrix $\boldsymbol{R}$ [20]. Finally, the poles in each region can be obtained by applying a root-finding algorithm to the denominator polynomial of (2).

In order to approximate the frequency characteristics for wide bandwidth, poles in every region are collected as the transfer function of all regions. As a result, Y_{ij} is expressed as follows:

$$Y_{ij}(s) = k_0 + \sum_{l=1}^{N_s} \frac{k_l^s}{s - p_l^s} + \sum_{l=1}^{N_c} \left\{ \frac{k_l^c}{s - p_l^c} + \frac{\overline{k}_l^c}{s - \overline{p}_l^c} \right\} \tag{4}$$

where k_0 is direct coupling, p^s and p^c are single poles and conjugate pairs, k^s and k^c are residues for each pole, and N_s and N_c are the numbers of single poles and conjugate pairs. Note that poles and residues in (4) are complex. Equation (5) is then derived to treat these imaginary parts as real numbers.

$$Y_{ij}(\overline{s}) = k_0 + \sum_{l=1}^{N_s} \frac{k_l^s}{\overline{s} - p_l^s} + \sum_{l=1}^{N_c} \left\{ \frac{k_l^c}{\overline{s} - p_l^c} + \frac{\overline{k}_l^c}{s - \overline{p}_l^c} \right\}. \tag{5}$$

Adding (4) and (5), and subtracting (5) from (4)

$$\begin{aligned} 2\mathrm{Re}Y_{ij}(j\omega) &= 2k_0 + 2\sum_{l=1}^{N_s} \frac{-\mathrm{Re}p_l^s}{\mathrm{Re}^2 p_l^s + \omega^2}\,\mathrm{Re}k_l^s \\ &\quad + 2\sum_{l=1}^{N_c} \left\{ \left(\frac{-\mathrm{Re}p_l^c}{\mathrm{Re}^2 p_l^c + (\omega - \mathrm{Im}p_l^c)^2} + \frac{-\mathrm{Re}p_l^c}{\mathrm{Re}^2 p_l^c + (\omega + \mathrm{Im}p_l^c)^2} \right) \mathrm{Re}k_l^c \right. \\ &\quad \left. + \left(\frac{\omega - \mathrm{Im}p_l^c}{\mathrm{Re}^2 p_l^c + (\omega - \mathrm{Im}p_l^c)^2} + \frac{-(\omega + \mathrm{Im}p_l^c)}{\mathrm{Re}^2 p_l^c + (\omega + \mathrm{Im}p_l^c)^2} \right) \mathrm{Im}k_l^c \right\} \end{aligned} \tag{6}$$

$$\begin{aligned} 2\mathrm{Im}Y_{ij}(j\omega) &= 2\sum_{l=1}^{N_s} \frac{-\omega}{\mathrm{Re}^2 p_l^s + \omega^2}\,\mathrm{Re}k_l^s \\ &\quad + 2\sum_{l=1}^{N_c} \left\{ \left(\frac{-(\omega - \mathrm{Im}p_l^c)}{\mathrm{Re}^2 p_l^c + (\omega - \mathrm{Im}p_l^c)^2} + \frac{-(\omega + \mathrm{Im}p_l^c}{\mathrm{Re}^2 p_l^c + (\omega + \mathrm{Im}p_l^c)^2} \right) \mathrm{Re}k_l^c \right. \\ &\quad \left. + \left(\frac{-\mathrm{Re}p_l^c}{\mathrm{Re}^2 p_l^c + (\omega - \mathrm{Im}p_l^c)^2} + \frac{\mathrm{Re}p_l^c}{\mathrm{Re}^2 p_l^c + (\omega + \mathrm{Im}p_l^c)^2} \right) \mathrm{Im}k_l^c \right\} \end{aligned} \tag{7}$$

can be derived, respectively, where $s = j\omega$, $k_l^s = \mathrm{Re}k_l^s$, $p_l^s = \mathrm{Re}p_l^s$, $k_l^c = \mathrm{Re}k_l^c + j\mathrm{Im}k_l^c$, and $p_l^c = \mathrm{Re}p_l^c + j\mathrm{Im}p_l^c$. Also, the equation at the origin ($s = 0$) is obtained by

$$Y_{ij}(0) = \sum_{l=1}^{N_s} \frac{-\mathrm{Re}l_l^s}{\mathrm{Re}p_l^s} + \sum_{l=1}^{N_c} \left\{ \frac{-2\mathrm{Re}p_l^c}{\mathrm{Re}^2 p_l^c + \mathrm{Im}^2 p_l^c}\,\mathrm{Re}k_l^s + \frac{-2\mathrm{Im}p_l^c}{\mathrm{Re}^2 p_l^c + \mathrm{Im}^2 p_l^c}\mathrm{Im}k_l^c \right\}. \tag{8}$$

Therefore, by deriving (6) and (7) of H frequency points excluding $s = 0$, (9) can be obtained, which is the matrix form, as

$$\boldsymbol{P}\boldsymbol{k} = \boldsymbol{y} \tag{9}$$

where

$$\begin{aligned} \boldsymbol{k} &= \begin{bmatrix} k_0 & \mathrm{Re}k_1^s & \cdots & \mathrm{Re}k_{N_s}^s & \mathrm{Re}k_1^c & \mathrm{Im}k_1^c \\ & \cdots & \mathrm{Re}k_{N_c}^c & \mathrm{Im}k_{N_c}^c \end{bmatrix}^T \\ \boldsymbol{y} &= [Y_{ij}(0) \quad 2\mathrm{Re}Y_{ij}(j\omega_1) \quad 2\mathrm{Im}Y_{ij}(j\omega_1) \\ &\quad \cdots \quad 2\mathrm{Re}Y_{ij}(j\omega_M) \quad 2\mathrm{Im}Y_{ij}(j\omega_M)]^T \end{aligned}$$

and $\boldsymbol{P}$ is the $(2H + 1) \times (1 + N_s + 2N_c)$ coefficient matrix, which is constructed by (6) and (7). By solving (9) for $\boldsymbol{k}$, Y_{ij} can be expressed as the transfer function with poles and residues. However, the poles, which are obtained by solving (9) for every region, can contain a duplicate pole and some undesirable ones. Therefore, it is necessary to select the dominant poles.

III. Selection of Dominant Poles by MIMO Type of SOLS Method

The matrix $\boldsymbol{P}$ of (9) contains some undesirable poles because the transfer function includes all poles that are obtained by dividing the frequency region. We then select the dominant poles with the SOLS method. By using this method, we can extract the dominant poles with orthogonalization in the QR decomposition.

The matrix $\boldsymbol{P}$ in (9) is expressed as

$$\boldsymbol{P} = \boldsymbol{W}\boldsymbol{A} \tag{10}$$

by the QR decomposition, where $\boldsymbol{W}$ is the $(2H+1)\times Q$ matrix with $Q(=1+N_s+2N_c)$ orthogonal columns and $\boldsymbol{A}$ is the $Q\times Q$ upper triangular matrix. In the SOLS method, residual vector $\boldsymbol{r}$ is defined as follows:

$$\boldsymbol{r} = \boldsymbol{y} - \boldsymbol{P}\boldsymbol{k} = \boldsymbol{y} - (\boldsymbol{P}\boldsymbol{A}^{-1})(\boldsymbol{A}\boldsymbol{k}) = \boldsymbol{y} - \boldsymbol{W}\boldsymbol{g} \tag{11}$$

and

$$\boldsymbol{g} = \boldsymbol{A}\boldsymbol{k} = \boldsymbol{D}^{-1}\boldsymbol{W}^{T}\boldsymbol{y} \tag{12}$$

where $\boldsymbol{D}$ is the positive diagonal matrix, which is given by $\boldsymbol{W}^{T}\boldsymbol{W}$, namely, the solution $\boldsymbol{k}$ of (9) is given by

$$\boldsymbol{k} = \boldsymbol{A}^{-1}\boldsymbol{g}. \tag{13}$$

Note that the residual $\boldsymbol{r}$ of (11) must be efficiently reduced in order to extract the dominant residues in (13). Here, the sum of squares of $\boldsymbol{y}$ is defined by

$$\langle \boldsymbol{y}, \boldsymbol{y}\rangle = \sum_{k=1}^{Q} g_k g_k \langle \boldsymbol{w}_k, \boldsymbol{w}_k\rangle + \langle \boldsymbol{r}, \boldsymbol{r}\rangle \tag{14}$$

where the symbol $\langle\cdot,\cdot\rangle$ denotes the inner product and $\boldsymbol{w}_i$ is the column vector of $\boldsymbol{W}$. As a result, the total least-square error normalized by $\langle \boldsymbol{y}, \boldsymbol{y}\rangle$ is written by

$$\frac{\langle \boldsymbol{r}, \boldsymbol{r}\rangle}{\langle \boldsymbol{y}, \boldsymbol{y}\rangle} = 1 - \sum_{k=1}^{Q} \frac{g_k g_k \langle \boldsymbol{w}_k, \boldsymbol{w}_k\rangle}{\langle \boldsymbol{y}, \boldsymbol{y}\rangle} = 1 - \sum_{k=1}^{Q} f_k. \tag{15}$$

Since the left-hand side of (15) is positive, the second term of the right-hand side of (15) takes $[0, 1]$. Since the column, which maximizes f_i, minimizes the residual vector $\boldsymbol{r}$, this is the column corresponding to the dominant pole. When we perform the QR decomposition of (9), we orthogonalize the column, which maximizes f_i, in rotation. These procedures are iterated until the residual becomes less than a small value δ. The remaining columns are then regarded as undesirable poles. As a result, the orthogonal matrix, which has only the columns corresponding to dominant poles, is derived.

However, in this procedure, the more the number of ports increases, the more the simulation cost increases because each element of admittance parameters requires to repeat the same procedure. Therefore, we expand this method to the MIMO type of approximation. In our method, (9) is expressed as

$$\boldsymbol{P}\boldsymbol{K} = \boldsymbol{Y} \tag{16}$$

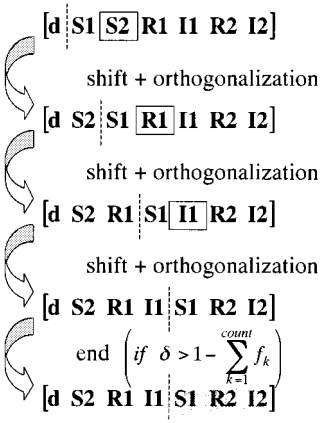

Fig. 1. Orthogonalization process for generating $\boldsymbol{W}$ from $\boldsymbol{P}$.

where

$$\boldsymbol{K} = [\boldsymbol{k}_{11} \quad \boldsymbol{k}_{12} \quad \cdots \quad \boldsymbol{k}_{nn}]$$
$$\boldsymbol{Y} = [\boldsymbol{y}_{11} \quad \boldsymbol{y}_{12} \quad \cdots \quad \boldsymbol{y}_{nn}]$$

where n is the number of ports. Our method achieves a MIMO type of approximation by selecting the common dominant poles from all of the poles that are obtained from diagonal elements. As a result, f_i in (15) is replaced by the norm of all elements as follows:

$$f_k = \frac{1}{N}\sqrt{\sum_{i=1}^{n}\sum_{j=1}^{n}\left(\frac{g_{ij,k}g_{ij,k}\langle \boldsymbol{w}_k, \boldsymbol{w}_k\rangle}{\langle \boldsymbol{y}_{ij}, \boldsymbol{y}_{ij}\rangle}\right)^2} \tag{17}$$

where the subscript ij indicates the element of matrix and N is the number of elements $(= n\times n)$. Our method is summarized in the following steps.

- Step 1) Calculate (17) for each column of the real part of the matrix $\boldsymbol{P}$.
- Step 2) Select and shift the column, which maximizes (17).
- Step 3) Orthogonalize for the column obtained at Step 2.
- Step 4) If the column obtained at Step 2 corresponds to single pole, go to Step 6, or else shift the column, which corresponds to the imaginary part.
- Step 5) Orthogonalize for the column obtained at Step 4.
- Step 6) If the sum of f_k for the columns, which are selected, satisfies the following condition (18), go to Step 7, or else exclude these from $\boldsymbol{P}$, and repeat Steps 1–6:

$$\delta > 1 - \sum_{k=1}^{\text{count}} f_k \tag{18}$$

  where $count$ is the number of columns that are selected.
- Step 7) Derive the residues.

Here, the orthogonalization process of our method is explained using the simple matrix shown in Fig. 1, where $\boldsymbol{d}$ is direct coupling, $\boldsymbol{S}$ is single pole, and $\boldsymbol{R}$ and $\boldsymbol{I}$ are real and imaginary parts of conjugate poles, respectively. First, f_k for each column of real part in the matrix $\boldsymbol{P}$ is calculated. If $\boldsymbol{S}2$ is maximum, $\boldsymbol{S}2$ is shifted and orthogonalized. In the next step, we calculate f_k for each column of real part excluding $\boldsymbol{S}2$. If

$\boldsymbol{R}1$ is selected, it is shifted and orthogonalized similarly to the above process. Since $\boldsymbol{I}1$ is the imaginary part of $\boldsymbol{R}1$, which forms conjugate poles, $\boldsymbol{I}1$ is inevitably selected in the next step. These procedures are iterated until the residual becomes less than a small value δ. The remaining columns are then regarded as undesirable poles, and the procedure is completed. As a result, the orthoganal matrix $\boldsymbol{W}$ and the upper triangular matrix $\boldsymbol{A}$, which have only the columns corresponding to dominant poles, are derived. In addition, the matrix $\boldsymbol{K}$ corresponding to the residues can be obtained by (13).

Finally, the following transfer function for admittance parameter:

$$Y_{ij}(s) = k_0 + \sum_{l=1}^{M} \frac{k_l}{s - p_l} \tag{19}$$

is obtained, where $p_l (l = 1, \ldots, M)$ are the M accurate poles and $k_l (l = 1, \ldots, M)$ are the accurate residues corresponding to the poles.

In our method, the dominant poles and residues of each element are determined at once. Therefore, the transfer function can be derived quickly.

IV. Synthesis of the Time-Domain Model

From (19), the time-domain model can be derived easily [14]. First, the terminal current is given by

$$I(s) = Y(s)V(s) = \sum_{l=1}^{M} \frac{k_l}{s - p_l} V(s). \tag{20}$$

Equation (20) is then reformulated as

$$I(s) = \sum_{l=1}^{M} k_l X_l(s) \tag{21}$$

where

$$X_l(s) = \frac{V(s)}{s - p_l}. \tag{22}$$

Equations (21) and (22) can be transformed into the time-domain expressions as

$$i(t) = \sum_{l=1}^{M} k_l x_l(t) \tag{23}$$

$$\frac{d}{dt} x_l(t) = p_l x_l(t) + v(t). \tag{24}$$

With (23) and (24), the voltage and current responses of the lines can be simulated using conventional circuit simulators.

V. Numerical Results

We have tried to synthesize the macromodels from the example circuit boards and performed transient simulation in order to verify the validity and efficiency of the proposed method.

Example 1: We modeled the interconnect using sampled data, which were obtained from the PCB shown in Fig. 2, and compared with the original frequency characteristics which

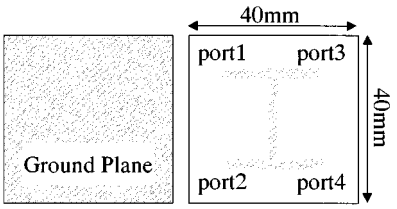

Fig. 2. Example PCB (a). (a) Bottom surface. (b) Top surface.

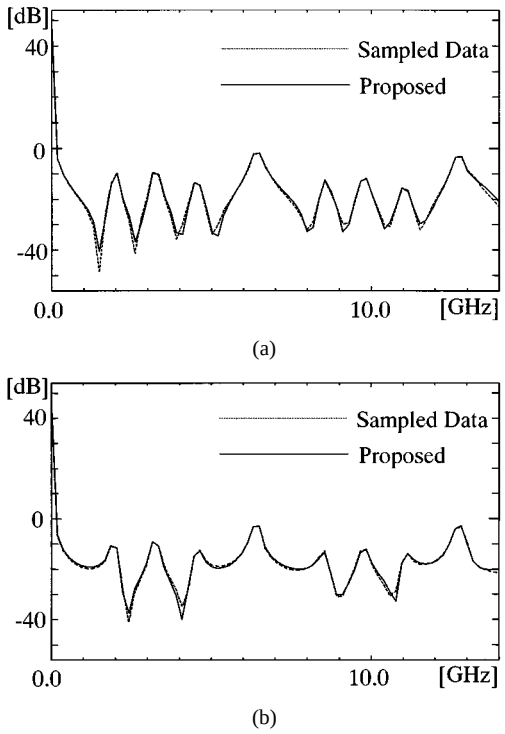

Fig. 3. Frequency responses of the example line. (a) Gain of Y_{11}. (b) Gain of Y_{24}.

indicate sampled data. Fig. 2 shows a PCB that consists of two layers, where one is the ground plane and the other is the signal plane with copper lines. In this PCB (a), the 0.1-mm distance between the bottom and top surfaces is filled with medium of permittivity $\epsilon_r = 4.3$. The sampled data have been extracted by the FFT of the impulse responses analyzed by the FDTD method [8], which is one of the full-wave analysis. The spatial steps used in the FDTD simulation are $\Delta x = \Delta y = 0.8$ mm and $\Delta z = 0.1$ mm, and the total mesh dimensions are $50 \times 50 \times 13$ in x-, y-, and z-directions, respectively. In the FDTD simulation to obtain the sampled data, the absorbing boundary condition of Higdon has been applied. In Fig. 3, the dotted line shows the sampled data, which are extracted by FDTD-based simulation with the above conditions. The frequency characteristics of admittance parameters Y_{11} and Y_{24}, which are approximated by the proposed method using the sampled data, are denoted by a solid line in Fig. 3. In our method, the frequency band is divided into 17 regions (with overlapping of each region not to miss the dominant poles) and 408 poles are obtained from diagonal elements. Finally, our reduction algorithm reduced the number of poles from 408 to 13.

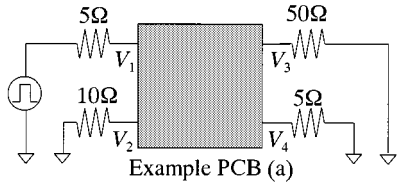

Fig. 4. Example circuit with PCB (a) and linear lumped elements.

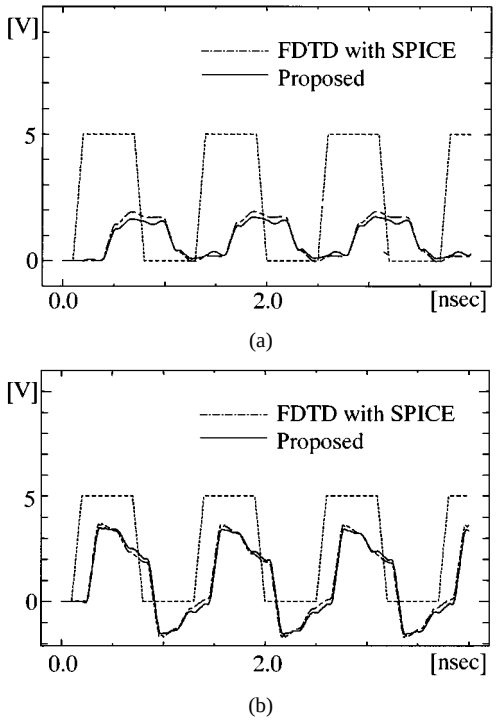

Fig. 5. Transient voltage waveforms of the example circuit in Fig. 4. (a) Response of V_2. (b) Response of V_3.

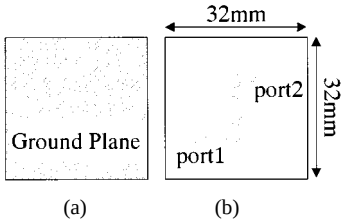

Fig. 6. Example PCB (b). (a) Bottom surface. (b) Top surface.

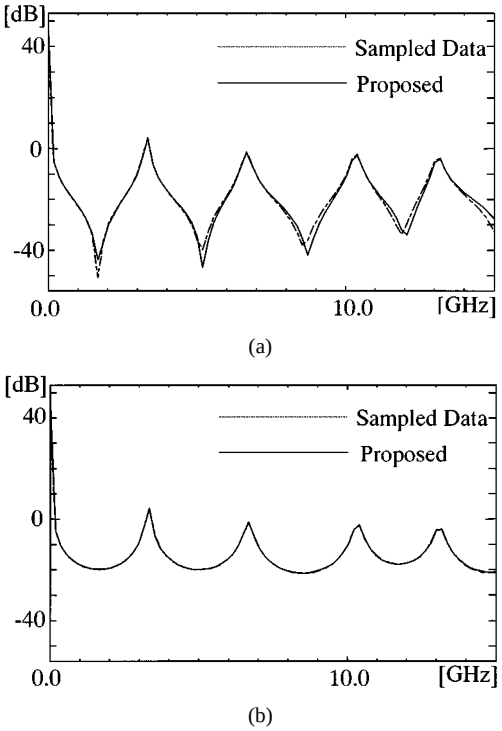

Fig. 7. Frequency responses of the example line. (a) Gain of Y_{11}. (b) Gain of Y_{12}.

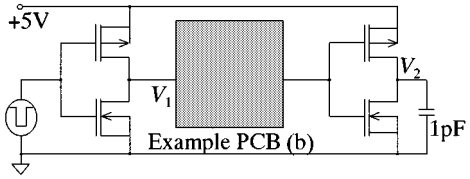

Fig. 8. Example circuit with PCB (b) and lumped elements.

Next, we simulated the transient response of the network, as illustrated in Fig. 4, which consists of the example PCB (a) shown in Fig. 2 and linear lumped elements using a SPICE-like simulator with the macromodel having 400 (25×16) poles. A method combining the FDTD method with SPICE was used for comparison. The transient output response obtained by the macromodel matches the result by the FDTD method with SPICE simulation, as shown in Fig. 5.

Example 2: We modeled the interconnect using sampled data, which were obtained from the PCB (b), shown in Fig. 6, and compared with the original frequency characteristics, which indicate sampled data. The example PCB (b) consists of signal and ground planes with copper, and 0.1-mm distance between these planes is filled with medium of permittivity $\epsilon_r = 4.3$. In the FDTD simulation to extract the sampled data, the spatial steps are $\Delta x = \Delta y = 0.8$ mm and $\Delta z = 0.1$ mm and the total mesh dimensions are $40 \times 40 \times 13$ in x-, y-, and z-directions, respectively. The frequency characteristics of admittance parameters Y_{11} and Y_{12}, which are approximated by our method using the sampled data, are shown in Fig. 7, where our reduction algorithm reduced the number of poles from 204 to 8. We also simulated the transient response of the network, as illustrated in Fig. 8, which consists of the example PCB (b), shown in Fig. 6, and linear and nonlinear lumped elements using a SPICE-like simulator with the macromodel having 60 (15×4) poles. The transient output response obtained by the macromodel matches the result by the FDTD method with SPICE simulation, as shown in Fig. 9.

Finally, comparison of CPU times required for each simulation is listed in Tables I and II. Table I displays that our approach to synthesize the macromodel is much faster than previous method [13], which indicates the SISO type of adaptive least-square method. In this comparison, the CPU cost for synthesis includes the time to calculate poles from sampled data using the least-square method and to select the dominant poles. Table II indicates that our SPICE-like simulator with the macromodel is much faster than the conventional FDTD method with SPICE simulation.

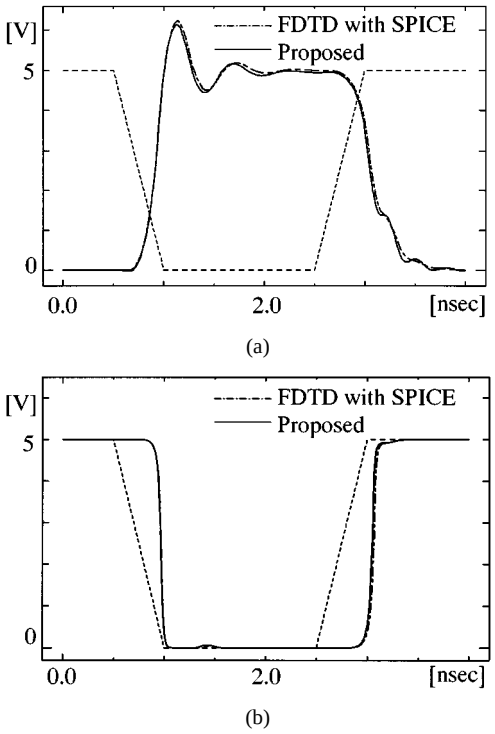

Fig. 9. Transient voltage waveforms of the example circuit in Fig. 8. (a) Response of V_1. (b) Response of V_2.

TABLE I
COMPARISON OF CPU TIMES FOR SYNTHESIS

	Example 1	Example 2
conventional	138.49 sec	34.46 sec
proposed	79.42 sec	22.57 sec

TABLE II
COMPARISON OF CPU TIMES FOR TRANSIENT SIMULATION

	Example 1	Example 2
FDTD with SPICE	876.53 sec	558.49 sec
proposed	8.35 sec	5.01 sec

VI. CONCLUSIONS

In this paper, we have proposed an efficient synthesis method of interconnect networks characterized by sampled data. We have described the model order-reduction technique by the MIMO type of SOLS method to reduce simulation cost. Numerical examples have been given to demonstrate the accuracy and efficiency of the proposed method.

In addition, since passivity of macromodels is a critical issue with transient analysis, several techniques [18], [19], which consider this problem, have been proposed. In these techniques, passivity of macromodels is preserved during reduction of the original MNA matrices whose passivity is ensured with congruence transformations. However, it is difficult to consider the passivity problem in this paper because the sampled data do not always ensure passivity. Preservation of passivity is of importance in future work.

REFERENCES

[1] F. Y. Chang, "The generalized method of characteristics for the waveform relaxation analysis of lossy coupled transmission lines," *IEEE Trans. Microwave Theory Tech.*, vol. 37, pp. 2028–2038, Dec. 1989.
[2] E. C. Chiprout and M. S. Nakhla, "Analysis of interconnect network using complex frequency hopping (CFH)," *IEEE Trans. Computer-Aided Design*, vol. 14, pp. 186–200, Feb. 1995.
[3] T. Watanabe and H. Asai, "Relaxation-based transient analysis of lossy coupled transmission lines circuits using delay evaluation technique," *IEICE Trans. Fund.*, vol. E81-A, no. 6, pp. 1055–1062, June 1998.
[4] D. H. Xie and M. S. Nakhla, "Delay and crosstalk simulation of high-speed VLSI interconnects with nonlinear terminations," *IEEE Trans. Computer-Aided Design*, vol. 12, pp. 1798–1811, Nov. 1993.
[5] K. S. Yee, "Numerical solution of initial boundary value problems involving Maxwell's equations in isotropic media," *IEEE Trans. Antennas Propagat.*, vol. AP-14, pp. 302–307, May 1966.
[6] W. K. Gwarek, "Analysis of arbitrarily shaped two-dimensional microwave circuits by finite-difference time-domain method," *IEEE Trans. Microwave Theory Tech.*, vol. 36, pp. 738–744, Apr. 1988.
[7] D. M. Sheen *et al.*, "Application of the three-dimensional finite-difference time-domain method to the analysis of planar microstrip circuits," *IEEE Trans. Microwave Theory Tech.*, vol. 38, pp. 849–857, July 1990.
[8] T. Watanabe and H. Asai, "Synthesis of time-domain models for interconnects having 3-D structure based on FDTD method," *IEEE Trans. Circuits Syst. II*, vol. 47, pp. 302–305, Apr. 2000.
[9] W. T. Beyene and J. Schutt-Aine, "Efficient transient simulation of high-speed interconnects characterized by sampled data," *IEEE Trans. Comp., Packag., Manufact. Technol. B*, vol. 21, pp. 105–114, Feb. 1998.
[10] K. L. Choi, N. Na, and M. Swaminathan, "Characterization of embedded passives using macromodels in LTTC technology," *IEEE Trans. Comp., Packag., Manufact. Technol. B*, vol. 21, pp. 258–268, Aug. 1998.
[11] G. Zheng, Q. J. Zhang, M. S. Nahkla, and R. Achar, "An efficient approach for moment-matching simulation of linear subnetworks with measured or tabulated data," in *Proc. IEEE Int. Computer-Aided Design Conf.*, 1996, pp. 20–23.
[12] S. Chen, S. A. Billings, and W. Luo, "Orthogonal least squares methods and their application to nonlinear system identification," *Int. J. Control*, vol. 50, no. 5, pp. 1873–1896, 1989.
[13] Y. Tanji and M. Tanaka, "A new order-reduction method of interconnect networks characterized by sampled data via orthogonal least square algorithm," in *Proc. IEEE Int. Circuits Syst. Symp.*, vol. 5, June 1999, pp. 543–546.
[14] M. S. Nakhla, "Recent progress in modeling and simulation of high-speed VLSI interconnects," in *IEEE ICECS'96: Collection Four Tutorials*.
[15] M. Celik and A. C. Cangellaris, "Efficient transient simulation of lossy packaging interconnects using moment-matching techniques," *IEEE Trans. Comp., Packag., Manufact., Technol. B*, vol. 19, pp. 64–73, Feb. 1996.
[16] W. T. Beyene and J. E. Schutt-Ainé, "Accurate frequency-domain modeling and efficient circuit simulation of high-speed packaging interconnects," *IEEE Trans. Microwave Theory Tech.*, vol. 45, pp. 1941–1947, Oct. 1997.
[17] M. Suzuki, H. Miyashita, A. Kamo, T. Watanabe, and H. Asai, "A synthesis technique of time-domain interconnect models by MIMO type of adaptive least square method," in *Proc. IEEE 9th Elect. Performance Electron. Packag. Topical Meeting*, Oct. 2000, pp. 233–236.
[18] K. J. Kerns and A. T. Yang, "Stable and efficient reduction of large, multiport *RC* networks by pole analysis via congruence transformations," *IEEE Trans. Computer-Aided Design*, vol. 16, pp. 734–744, July 1997.
[19] A. Odabasioglu, M. Celik, and L. T. Pileggi, "PRIMA: Passive reduced-order interconnect macromodeling algorithm," *IEEE Trans. Computer-Aided Design*, vol. 17, pp. 645–654, Aug. 1998.
[20] H. R. Schwarz, *Numerical Analysis*. New York: Wiley, 1998.

Masaya Suzuki was born in Shizuoka Prefecture, Japan, in 1977. He received the B.E. degree from Shizuoka University, Hamamatsu, Japan, in 2000, and is currently working toward the M.E. degree in science and engineering at Shizuoka University.

His research interests include circuit simulation.

Hirofumi Miyashita was born in Nagano Prefecture, Japan, in 1977. He received the B.E. and M.E. degree from Shizuoka University, Shizuoka, Japan, in 1999 and 2001, respectively.

He is currently with the Matsushita Electric Industrial Company Ltd., Osaka, Japan.

Atsushi Kamo was born in Shizuoka Prefecture, Japan, in 1974. He received the B.E. and M.E. degree from Shizuoka University, Hamamatsu, Japan, in 1997 and 1999, respectively, and is currently working toward the Ph.D. degree in electronic science and technology at Shizuoka University.

His research interests include circuit simulation.

Takayuki Watanabe (M'99) was born in Shizuoka Prefecture, Japan, on June 5, 1972. He received the B.E., M.E., and Ph.D. degrees from Shizuoka University, Hamamatsu, Japan, in 1995, 1997, and 2000, respectively.

He is currently a Research Associate in the School of Administration and Informatics, University of Shizuoka. His research interests include VLSI–computer-aided design (CAD) algorithms and high-performance computing and communications.

Dr. Watanabe is a member of the Institute of Electronics, Information and Communication Engineers (IEICE), Japan.

Hideki Asai (M'91) received the B.E., M.E., and Ph.D. degrees in electrical engineering from Keio University, Yokohama, Japan, in 1980, 1982, and 1985, respectively.

In 1985, he was with the Department of Electrical and Electronics Engineering, Sophia University, Tokyo, Japan. He was a Visiting Professor at Carleton University, Ottawa, ON, Canada, and Santa Clara University, Santa Clara, CA (1999–2000). Since 1986, he has been with Shizuoka University, Hamamatsu, Japan, where he is currently a Professor involved with VLSI–CAD and electrical design automation (EDA), parallel computing systems, and neural networks.

Dr. Asai is a member of the IEEE Nonlinear Circuits and Systems Technical Committee. He was secretary for the IEEE Circuits and Systems Society Tokyo Chapter (1994–1995), and secretary of the Technical Group on Nonlinear Problems of the Institute of Electronics, Information and Communication Engineers (IEICE) (1997–1999). He was the recipient of the Research Encouragement Awards on the occasion of the Takayanagi anniversary, the 50th anniversary of the founding of the IEICE Tokai branch, and on the occasion of the Saitoh anniversary in 1988, 1989, and 1993, respectively.